RSC Advances

PAPER

View Article Online
View Journal | View Issue

Cite this: *RSC Adv.*, 2021, **11**, 36215

Determination of sodium and potassium ions in patients with SARS-Cov-2 disease by ion-selective electrodes based on polyelectrolyte complexes as a pseudo-liquid contact phase

Liubov V. Pershina,[a] Andrei R. Grabeklis,[bc] Ludmila N. Isankina,[d] Ekaterina V. Skorb *[a] and Konstantin G. Nikolaev *[a]

Nowadays, there are several methods for the detection of various bioelements during SARS-CoV-2. Many of them require special equipment, high expenses, and a long time to obtain results. In this study, we aim to use polyelectrolyte multilayers for robust carbon fiber-based potentiometric sensing to determine the ion concentration in human biofluids of COVID-19 patients. The polyethyleneimine/polystyrene sulfonate complex is hygroscopic and has the ability to retain counterions of inorganic salts. This fact makes it possible to create a flexible ionometric system with a pseudo-liquid connection. The formation of the polyethyleneimine/polystyrene sulfonate complex allows for the adhesion of a hydrophobic ion-selective membrane, and creates a Nernst response in a miniature sensor system. This approach discloses the development of miniaturized ion-selective electrodes and their future application to monitor analyte changes as micro and macroelement ions in the human body to identify correlation to SARS-CoV-2. An imbalance in the content of potassium and sodium in urine and blood is directly related to changes in the zinc content in patients with coronavirus. The proposed method for assessing the condition of patients will allow fast determination of the severity of the course of the disease.

Received 14th June 2021
Accepted 9th October 2021

DOI: 10.1039/d1ra04582b

rsc.li/rsc-advances

Introduction

The COVID-19 pandemic, known as the coronavirus pandemic, is a continuous world pandemic of coronavirus disease 2019 (COVID-19) induced by serious acute respiratory syndrome coronavirus 2 (SARS-CoV-2). There are numerous methods of coronavirus detection. Nowadays, quantitative reverse transcription-polymerase chain reaction (qRT-PCR) is the golden standard for the diagnosis and confirmation of the SARS-CoV-2 infection.[1] In addition, many other methods are being developed for more rapid and selective COVID-19 determination. There are approaches based on immunochromatographic detection,[2] mass-spectrometry-based methods,[3,4] and electrochemical methods with biosensors used for the rapid detection of SARS-CoV-2.[5–7]

Another importance that can be mentioned, there are electrolyte imbalances in human biofluids that can occur in any critical systemic illness.[8] Electrolyte imbalance can also be a considered evaluation indicator for revealing strategies for treating patients with COVID-19.[9] Earlier, it was reported various electrolyte anomalies for patients who progress towards the heavy form of SARS-CoV-2.[10] More characteristic is the change in the content of macroelement ions, such as potassium and sodium[10–12] and some trace elements, including zinc.[13,14] It was studied that electrolyte and trace element changes are related, and increasing or decreasing some of them affects the severity and COVID-19.[14] In addition, supplemental intake of these nutrients has been shown to increase the antiviral resistance to coronavirus infection.[15,16]

The virus infects the host by binding to the angiotensin-converting enzyme 2 receptors. Angiotensin-converting enzyme 2 receptors present in the kidneys and gastrointestinal tract, and kidneys and gastrointestinal tract damage arising from the virus can be seen in patients and can lead to acute conditions, for example, acute kidney injury and digestive problems for the patients.[17] Among the most easily detected indicators, the most promising for long-term monitoring are the content of electrolytes, sodium and potassium. Among patients hospitalized with COVID-19, dysnatremia is commonly present at admission, with hyponatremia being more prevalent

[a]*Infochemistry Scientific Center of ITMO University, 191002 Saint Petersburg, Russian Federation. E-mail: skorb@itmo.ru; kgnikolaev@itmo.ru*

[b]*World-Class Research Center "Digital Biodesign and Personalized Healthcare", Sechenov First Moscow State Medical University, Trubetskaya st., 8, 119991 Moscow, Russian Federation*

[c]*Peoples' Friendship University of Russia (RUDN University), Miklukho-Maklay st., 6, Moscow, 117198, Russian Federation*

[d]*Children's City Clinical Hospital, No. 5 named after N.F. Filatov, 192889 Saint Petersburg, Russian Federation*

than hypernatremia.[18] Serum sodium imbalance serves as a common characteristic feature and leads to severe illnesses, poor clinical outcome(s) and increased in-hospital mortality in COVID-19 patients.[19] The treatment of COVID-19 pneumonia in hospitals should provide sodium and potassium continuous monitoring because patients admitted with dysnatremia are at a higher risk for negative endpoints than those presenting with eunatremia.[20]

In the practice of the analysis of biological fluids for metal ions, almost all the spectroscopic methods for element analysis find use: atomic absorption spectrometry (AAS) in different modifications, inductively coupled plasma atomic emission spectrometry (ICP-AES), X-ray fluorescence analysis (XFA), and inductively coupled plasma mass spectrometry (ICP-MS).[21,22] Electrochemical detection methods, including ion-selective sensors, for ion determination have attracted attention due to the advantages of high sensitivity, miniaturization, ease of operation, and the ability of simultaneous multiion detection. Simultaneously, methods for electrode nanostructuring for making the electrochemical detection methods robust are of high priority. An outstanding trend is the modification of surfaces with supramolecular biomimetic structures. For example, polyelectrolyte complexes make it possible to create hydrogel layers with desired properties.[23,24] Organometallic frameworks, due to their properties, create interfaces for the determination of small molecules and heavy metals.[25–28]

In recent years for these purposes, fibrous textile materials are used as the basis for the electrode substrate due to their wearable property and biocompatibility.[29] Conductive fibrous materials, which include carbon fiber, are widely used in the field of electrochemistry due to their mobility, electrical conductivity, environmental resistance, and the possibility of low commercial cost. The possibility of using carbon adhesive tapes[30] and carbon fibers[31] was shown for the manufacturing of potentiometric devices based on ISEs. Cotton thread-based carbon black coated potentiometric sensors were found to have a widespread application for the multiplexed analysis of electrolytes and metabolites in blood.[32] Previously, we have developed a portative platform based on a carbon fiber electrode for Zn detection in blood and urine samples.[31]

We afforded the carbon fiber electrode as a substrate for the ion-selective electrode with pseudo-liquid junction. Previous studies have shown the possibility of immobilizing polyelectrolyte nanolayers on the surface of a carbon fiber.[31] This study demonstrates a new interface: hydrophobic carbon fiber – hydrophilic layers of polyelectrolytes – hydrophobic ion-selective membrane. This interface enables to propose the potential method of correlation for COVID-19 with electrochemical measurements using ion-selective electrodes to determine the sodium and potassium ion concentration change in urine and blood serum (Fig. 1).

Results and discussion

Desired electroanalytical characteristics were achieved using miniaturized ion-selective electrodes modified with polyelectrolytes.[30] The conducting materials, in particular different polyelectrolytes, are used as ion-to-electron transducers primarily for creating solid contact ion-selective electrodes.[33] However, the application of classical solid contact sensors with ion-selective membranes for the medicine area is difficult due to the necessary miniaturization of the design of problems with the stability and reproducibility of the signal.[34] The most difficult problem in the design of ion-selective electrodes is the increase in the charge transfer resistance. Additional limitations for measuring the electromotive force of an electrochemical cell are imposed using inexpensive high-resistive carbon-containing fibers. The difference between the resistance values of the carbon fiber and the commercial Ag/AgCl reference electrode can result in a "breakdown" in the electrochemical circuit, which causes an unstable analytical signal. The carbon fiber-based reference electrode creates a symmetrical interface. This approach ensures the stability of the measurement of the electromotive force. Therefore, the creation of ion-selective electrodes with a pseudo-liquid internal solution based on polyelectrolytes and carbon fiber solves the above problems. Polyelectrolytes are widespread in electrochemical sensor various materials to modification of sensing layers. These materials increase sensitivity, selectivity, and electronic bonds with the sensor substrate, and they can mediate electron transfer between an analyte and a transducer.[35] In addition, the conductive polymers have moderate biocompatibility, which allows using them in biosensing.[36] In this study, polyelectrolytes were applied as modifiers of the working surface by layer-by-layer (LbL) deposition. This approach based on the sequential deposition of oppositely charged molecules due to electrostatic interactions allows the formatting of ultrathin molecular films with a wide range of functional possibilities.[37] In addition, the LbL assembly was successfully implemented on cation exchange membranes.[38] This approach provides high stability during the sensor measurement and storage.[21]

As a conductive material, carbon fiber is an inexpensive, commercially available, and promising material for creating flexible devices. Also, carbon fiber materials promise good biocompatibility, which is essential to make biosensors.[39]

The electrode working surface was nanostructured with a polyelectrolyte multilayer by the LbL assembly. As polyelectrolytes, we set the poly(4-styrenesulfonate) (PSS) polyanion, a strong polyelectrolyte, and the poly(ethyleneimine) (PEI) polycation, which has a highly branched structure and a high density of positive charge, on a polymer base.[40,41] The layers of polyelectrolytes adsorbed on the carbon fiber surface form a pseudo internal solution and act as an ion-electronic transducer. The adsorbed layers of polyelectrolytes retain water and salts, which makes it possible to create the polyelectrolyte hydrogel on the surface of the carbon fiber. The schematic process of depositing polyelectrolytes on the carbon fiber is illustrated in Fig. 2. Well-resolved carbon fiber/polyelectrolyte complex/ion-selective membrane interfaces allow the detection of good adhesion of polyelectrolytes on the carbon fiber surface as well as good adhesion of the ion-selective membrane to the polyelectrolyte complex. PEI has a high affinity for potassium ions. This affinity is not explained by the charge compensation mechanism, but by the internal osmotic pressure

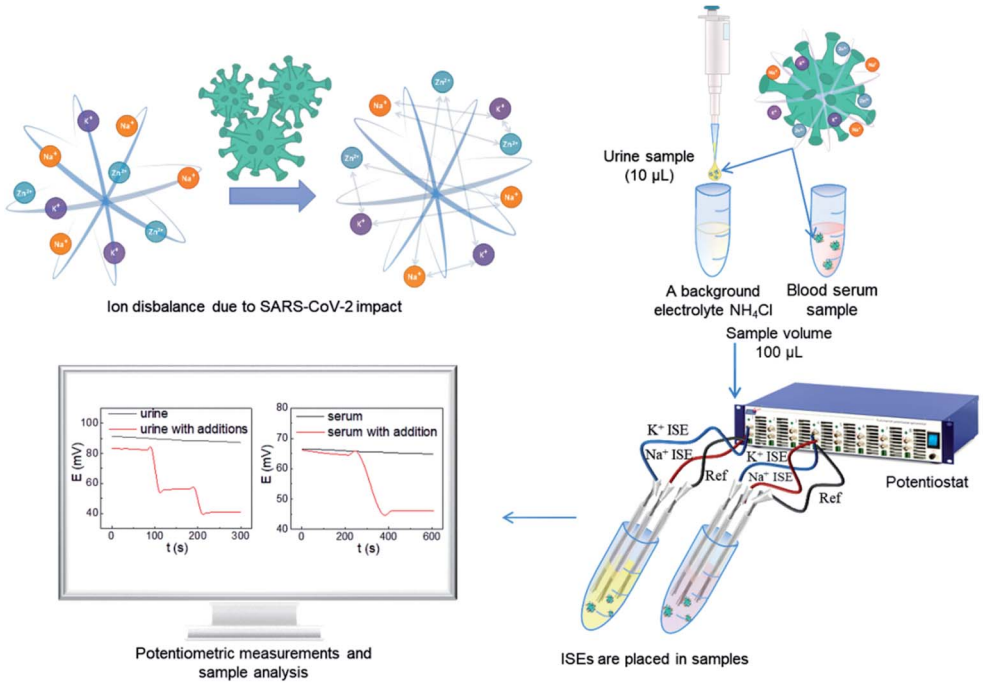

Fig. 1 Scheme of the electroanalysis of ions in blood and urine by ion-selective sensors.

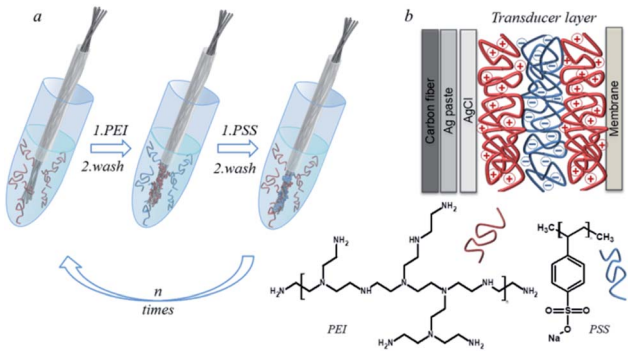

Fig. 2 The carbon fiber modification by the polyelectrolyte LbL assembly (a), common scheme of the ion-selective electrode (b).

that occurs in the polyethyleneimine layer.[42] When the next layer of PSS is applied to PEI, the complexation of polyelectrolytes occurs. In this case, a part of potassium ions is displaced, which is compensated by the fact that part of the groups of PSS is also compensated by potassium ions. Chloride ions are retained by the electrostatic compensation of the amino groups of PEI. The PEI/PSS layers of polyelectrolytes form a charge-compensated complex.[43] Thus, the carbon chains of the polyelectrolytes provide adhesion to the hydrophobic surface of the carbon fiber. Moreover, the resulting architecture of polyelectrolytes allows the deposition of a hydrophobic ion-selective membrane. In accordance with previous studies the optimal design of the polyelectrolyte membrane was selected, which contained 8 bilayers of PEI/PSS.[31] The mechanism proposed by us made it possible to create a pseudo-liquid internal reference electrode with a constant activity of potassium and chlorine ions, which is the main criterion for the operation of ion-selective electrodes with a liquid connection.

The adsorption of the polyelectrolyte layer on the carbon fiber surface was studied by scanning electron microscopy (Fig. 3). Different areas were examined at different magnifications, from 500 μm to 10 μm. The diameters of the carbon fibers were approximately 300 ± 50 μm, the sizes of internal inclusions along the periphery were about 5 ± 3 μm and clusters up to 20 ± 10 μm were observed in the central region. Individual fibers, spherical clusters, and cubic structures were seen as inclusions. Layers of the material with different contrast were found around the fiber perimeter.

It was assumed that the detected layers were Ag paste, ISM, and polyelectrolyte layer, which proved their adsorption on the fiber. Approximate thicknesses of the observed layers: polyelectrolyte layer −7 ± 3 μm, ISM −20 ± 5 μm, Ag paste −10 ± 5 μm. The microsized thickness of the polyelectrolyte complex indicates swelling, as well as effective adsorption on the surface of the hydrophobic carbon fiber electrode. The thickness of the ISM proved uniform adhesion on the surface of the

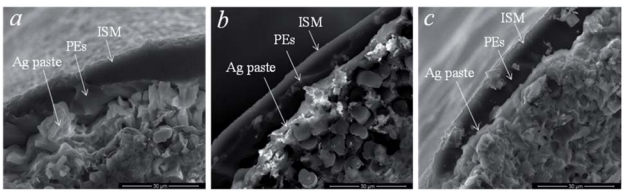

Fig. 3 The SEM images of the CF electrodes modified with polyelectrolytes before (a and b) and after (c) potentiometric measurements.

polyelectrolyte complex. The hydrophobic silver paste, due to its suitable viscosity, provided a comparable layer thickness, thus not being a resistance-limiting layer.

In particular cations, the potentiometric measurement of electrolytes occurs due to the presence of an ion-selective membrane, which includes an ionophore, which reversibly binds a specific ion.

In each experiment, potassium and sodium ISEs were immersed into solutions of the corresponding salts (KCl and NaCl, respectively). The concentration of the solution was changed in steps after each addition of the standard solution. The potential values were monitored continuously by a potentiostat. Electromotive force (EMF) was measured between the working ISE and a commercial Ag/AgCl reference electrode. Fig. 4(a and c) demonstrates the time diagrams of potentiometric response for the prepared carbon fiber-based ISMs of K and Na ions when the concentration of the primary analyte increased. The effect of layering in combination with an ion-selective membrane has been discussed previously.[44] However, a crosslinking method was used to enhance adhesion to the hydrophobic membrane. The data (Fig. 4) demonstrated the possibility of creating ion-selective sensors with a Nernst response based on the proposed interface.

The potassium ion concentration ranges from 1.9 to 4.0 mM and 3.5 to 5.5 in human urine and blood serum.[45] Na ion concentration is in the range of 78.0 to 130.0 mM and 136.0 to 145.0 mM in human urine and blood serum.[46] The sensitivities of both ISEs were in the range from 10^{-4} to 1 M (Fig. 4b and d) – limits of linearity (LOL). The limits of detection (LOD) and quantification (LOQ) were 2.7×10^{-5} and 8.9×10^{-5} for potassium and 2.1×10^{-5} and 6.9×10^{-5} for sodium, respectively. This allows to conclude that the electrodes provided necessary measurements in biological fluids. With the carbon fiber,[21] the normal blood serum zinc content (0.66 to 1.10 mcg mL^{-1}) (ppm)[47] can be measured, which is important for COVID-19. Here, we aimed at robust carbon fiber electrodes for sodium and potassium ions in biofluids. The methods of the LbL polyelectrolyte assembly allowed for achieving high sensitivity and selectivity together with a robust response. The obtained analytical characteristics proved the possibility of using a miniaturized ion-selective system with a pseudo-liquid compound for monitoring the content of potassium and sodium ions.

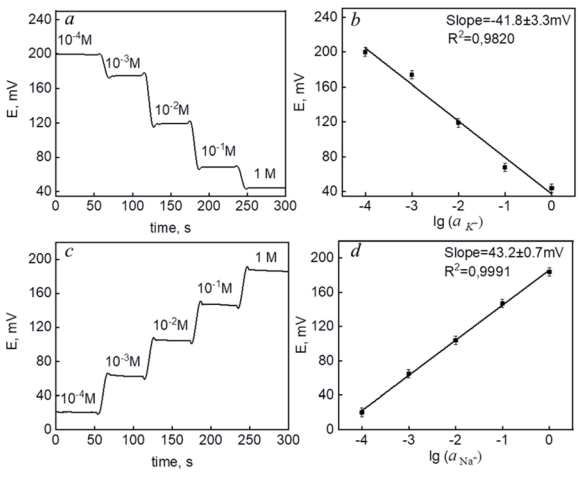

Fig. 4 Potentiometric response for potassium (a) and sodium ions (c) on ISEs and corresponding calibration plots after addition of the standard solution ($y = -41.8x + 37.4$, $n = 3$, $p = 0.95$; $y = 43.2x + 186.0$, $n = 3$, $p = 0.95$) (b and d).

Urine samples were prepared by previous dilution 10 times by 0.1 M NH_4Cl as a background electrolyte. Blood serum samples were measured without previous preparation. The results of the potentiometric measurements are demonstrated in Tables 1 and 2. Previously, representative studies were carried out to detect metal ions in human biological objects.[13] From the huge data,[13] we have selected the most representative ones for comparison with the proposed method.

It was detected that potassium content was below normal and sodium content was above normal in the studied samples. The low potassium content in human organisms (hypokalemia) has been referenced as a potential manifestation of COVID-19. Potassium deficiency has been a common electrolyte disturbance in hospitalized COVID-19 patients.[48] Measurement resulting from real blood serum and urine samples showed good correlation with the reference values. There was no influence of the matrix effect on the analytical signal. Even though the values obtained using ion-selective sensors were coarser than those obtained for the reference method, they were satisfactory for miniature sensor devices.

Normal blood serum potassium content is 136.5 to 214.5 μg mL^{-1} (ppm).[45]

Normal blood serum sodium content is 3128 to 3335 μg mL^{-1} (ppm).[46]

Normal urine potassium content is 1.9 to 4.0 mM.[45]

Normal urine sodium content is 78.0 to 130.0 mM.[46]

The level of sodium in humans is also an essential indicator of severity in COVID-19. It was discovered that hypernatremia is very common in severe COVID-19.[49] The increased incidence of hypernatremia seems to be associated with a significant water loss during the disease.[50] The results obtained indicated a correlation between micro and macro elements in the blood and urine of patients with coronavirus. An imbalance in the content of potassium and sodium in urine and blood is directly related to changes in the content of zinc in patients with coronavirus. The increased zinc content maybe because the patients were in severe and moderate degrees of the disease. Simultaneously, an imbalance of potassium and sodium indicates the stage of the disease.

The results obtained were in good agreement with those reported in the literature.[50] This, in turn, allows us to conclude

Table 1 Results of potassium and sodium concentration measurements in urine samples ($n = 3$, $p = 0.95$)

Urine sample	C_{K^+}, mmol L^{-1}	C_{K^+}, ppm	C_{Na^+}, mmol L^{-1}	C_{Na^+}, ppm
1	1.41 ± 0.27	55 ± 3	134.6 ± 0.4	3096 ± 28
2	1.81 ± 0.64	71 ± 2	154.7 ± 0.8	3557 ± 17
3	1.87 ± 0.57	73 ± 3	153.2 ± 0.5	3523 ± 25

Table 2 Results of potassium and sodium concentration measurements in blood serum samples ($n = 3$, $p = 0.95$)

Blood sample	C_{K^+}, mmol L^{-1}	C_{K^+}, ppm	C_{Na^+}, mmol L^{-1}	C_{Na^+}, ppm
1	3.25 ± 0.15	127 ± 4	214.8 ± 0.6	4940 ± 25
2	1.33 ± 0.24	52 ± 7	189.4 ± 0.9	4356 ± 37
3	1.42 ± 0.26	55 ± 2	190.5 ± 0.1	4381 ± 15

about the possibility of using the proposed sensors to determine the content of sodium and potassium in the blood and urine of patients with diagnosed coronavirus infection to assess their condition.

Experimental section

Materials and methods

Chemicals and materials. Urine samples were obtained from Children's City Clinical Hospital No. 5 named after N.F. Filatov (Saint Petersburg, Russian Federation). Blood serum samples were obtained from I.M. Sechenov First Moscow State Medical University (Moscow, Russian Federation). Valinomycin (potassium ionophore I), 4-tertbutylcalix[4]arene-tetraacetic acid tetraethyl ester (sodium ionophore X), potassium tetrakis(4-chlorophenyl)borate (KTpCIPB), 2-nitrophenyl octyl ether (*o*-NPOE), bis(2-ethylhexyl)sebacate, poly(vinyl chloride) high molecular weight (PVC), hyperbranched poly(ethyleneimine) (PEI, MW = ~750 000, 50% (w/v) solution), poly(sodium 4-styrenesulfonate) (PSS, MW = ~1 000 000), tetrahydrofuran solution (THF, 45% in H_2O) and sodium chloride (NaCl) were all purchased from Sigma-Aldrich(USA). Potassium chloride (KCl) and ammonium chloride (NH_4Cl) were purchased from Len-Reactiv (Russia). CFs with 250 g m^{-2} of area density were produced by M-Carbo (Minsk, Belarus). Silver conductive glue (Kontakt, Keller) was purchased from local stores. All solutions were prepared using DI water (18.0 MΩ cm, Milli-Q gradient system, Millipore, Burlington, MA).

Fabrication of the ISM

The potassium ISM containing 1.0 wt% of valinomycin (potassium ionophore I), 0.5 wt% of potassium tetrakis(4-chlorphenyl)borate, 49.0 wt% of PVC, and 49.5 wt% of bis(2-ethylhexyl)sebacate. The sodium ISM containing 0.7 wt% of 4-tertbutylcalix[4]arene-tetraacetic acid tetraethyl ester (sodium ionophore X), 0.2 wt% of potassium tetrakis(4-chlorphenyl) borate, 33.0 wt% of PVC, and 66.1 wt% of 2-nitrophenyl octyl ether. The membranes were prepared by dissolving the mixture into 1.5–2 mL of THF. ISM coatings were prepared by ten-fold drop-casting onto the electrode. The membranes were dried for 24 h. The electrodes were conditioned in a proper saline solution for 24 h before the measurements.

Modification of the ISEs

The nanostructuring of the electrode surface was carried out by the layer-by-layer deposition of polyelectrolyte solutions. A polyionic film was applied to the working surface of the carbon fiber over a layer of silver. Layers of positively charged PEI and negatively charged PSS were applied from water solution with a polyelectrolyte concentration of 2 mg mL^{-1} to modify the sodium electrode and from the solution of 1 M KCl for potassium. For the deposition of each layer, the surface was kept for 30 s at room temperature in a polyelectrolyte solution. The fiber was washed with water between the depositions of the polyelectrolyte layers.

Potentiometric measurements

Measurements of the electromotive force were carried out using a Potentiostat/Galvanostat SP-50 (Electrochemical Instruments, Russia) in a standard two-electrode cell at room temperature (23 °C). The CF-based ISE was used as the working electrode and an Ag/AgCl commercial electrode as the reference one.

Scanning electron microscopy

The measurements were carried out on a scanning electron microscope (SEM) Inspect (USA, FEI) in a vacuum at a pressure of about 10^{-3} to 10^{-4} [Pa] and an accelerating voltage of 20 [kV]. Carbon fibers were placed with their end face towards the scanning plane (before that, a fresh cut was made in the transverse plane to visualize the internal structure) to study the polyelectrolyte's internal structure; a conductive carbon adhesive tape was used for fixation. The measurements were carried out with thermionic emission of electrons from the W cathode and detection of secondary electrons (Everhart–Thornley detector).

Real sample object ethical statement

The present study was performed in agreement with the ethical standards set in the Declaration of Helsinki (1964) and its later amendments. Informed consent was obtained from all persons, who were involved in the study.

Conclusions

We have shown the possibility of measuring the content of potassium and sodium ions in urine and blood without preliminary sample preparation due to use of methods for the surface nanostructuring of carbon fiber *via* LbL polyelectrolyte complexation. The proposed method for creating a charge-compensated polyelectrolyte complex made it possible to improve the adhesion of a hydrophobic ion-selective membrane on the polyelectrolyte-modified surface. The Nernst-responsive interface was demonstrated for the miniature sensor system. The sensor system based on a polyelectrolyte complex showed the possibility of simultaneous detection of potassium and sodium ions. Analysis of real samples showed no influence of the matrix effect on the analytical signal. Biomimetic and supramolecular architectures will increasingly be used in the future to create complex interfaces with predicted properties. In addition, correlating sodium and potassium as well as the previously shown blood zinc allowed measuring ions without expensive instruments. In the future, measurements using electrodes without preliminary sample preparation can reduce

the analysis time. The use of miniature ion-selective sensors will allow detecting the disease itself and the degree of its course. In turn, this will provide a fast and preventive medical care. Miniature ion-selective systems will enable the collection of large data in the future, and, in combination with trace element data, enable early diagnosis and rapid monitoring in particular during pandemic situations.

Conflicts of interest

The authors declare no conflict of interest.

Acknowledgements

The authors acknowledge the RSF grant no. 19-73-00315 for the financial support.

Notes and references

1 K. A. Khan and P. Cheung, *R. Soc. Open Sci.*, 2020, **7**(6), 200636.
2 Y. Pan, X. Li, G. Yang, J. Fan, Y. Tang, J. Zhao, X. Long, S. Guo, Z. Zhao, Y. Liu, H. Hu, H. Xue and Y. Li, *J. Infect.*, 2020, **81**, e28–e32.
3 E. N. Nikolaev, M. I. Indeykina, A. G. Brzhozovskiy, A. E. Bugrova, A. S. Kononikhin, N. L. Starodubtseva, E. V. Petrotchenko, G. I. Kovalev, C. H. Borchers and G. T. Sukhikh, *J. Proteome Res.*, 2020, **19**, 4393–4397.
4 N. L. Dollman, J. H. Griffin and K. M. Downard, *ACS Infect. Dis.*, 2020, **6**, 3269–3276.
5 H. Yousefi, A. Mahmud, D. Chang, J. Das, S. Gomis, J. B. Chen, H. Wang, T. Been, L. Yip, E. Coomes, Z. Li, S. Mubareka, A. McGeer, N. Christie, S. Gray-Owen, A. Cochrane, J. M. Rini, E. H. Sargent and S. O. Kelley, *J. Am. Chem. Soc.*, 2021, **143**(4), 1722–1727.
6 B. Mojsoska, S. Larsen, D. A. Olsen, J. S. Madsen, I. Brandslund and F. A. Alatraktchi, *Sensors*, 2021, **21**(2), 390.
7 H. Xi, M. Juhas and Y. Zhang, *Biosens. Bioelectron.*, 2020, **167**, 112494.
8 M. Bansal, *Diabetes Metab. Syndr.: Clin. Res. Rev*, 2020, **14**, 247–250.
9 W. Wang, Z. Zhao, X. Liu, G. Liu, D. Xie, Z. Xu, J. Zhao and J. Zhang, *J. Clin. Lab. Anal.*, 2020, **34**, 1–8.
10 G. Lippi, A. M. South and B. M. Henry, *Ann. Clin. Biochem.*, 2020, **57**, 262–265.
11 H. De Carvalho, M. C. Richard, T. Chouihed, N. Goffinet, Q. Le Bastard, Y. Freund, A. Kratz, M. Dubroux, D. Masson, L. Figueres and E. Montassier, *Intern. Emerg. Med.*, 2021, 1–6.
12 M. Ciaccio and L. Agnello, *Diagnosis*, 2020, **7**, 365–372.
13 A. V. Skalny, P. S. Timashev, M. Aschner, J. Aaseth, L. N. Chernova, V. E. Belyaev, A. R. Grabeklis, S. V Notova, R. Lobinski, A. Tsatsakis, A. A. Svistunov, V. V Fomin, A. A. Tinkov and P. V Glybochko, *Metabolites*, 2021, **11**(4), 244.
14 M. Taheri, A. Bahrami, P. Habibi and F. Nouri, *Biol. Trace Elem. Res.*, 2021, **199**, 2475–2481.
15 J. Alexander, A. Tinkov, T. A. Strand, U. Alehagen, A. Skalny and J. Aaseth, *Nutrients*, 2020, **12**(8), 2358.
16 A. V. Skalny, L. Rink, O. P. Ajsuvakova, M. Aschner, V. A. Gritsenko, S. I. Alekseenko, A. A. Svistunov, D. Petrakis, D. A. Spandidos, J. Aaseth, A. Tsatsakis and A. A. Tinkov, *Int. J. Mol. Med.*, 2020, **46**, 17–26.
17 M. Pourfridoni, S. M. Abbasnia, F. Shafaei, J. Razaviyan and R. Heidari-Soureshjani, *BioMed Res. Int.*, 2021, 6667047.
18 J. S. Hirsch, N. N. Uppal, P. Sharma, Y. Khanin, H. H. Shah, D. A. Malieckal, A. Bellucci, M. Sachdeva, H. Rondon-Berrios, K. D. Jhaveri, S. Fishbane and J. H. Ng, *Nephrol., Dial., Transplant.*, 2021, **383**, 1–4.
19 W. Hu, X. lv, C. Li, Y. Xu, Y. Qi, Z. Zhang, M. Li, F. Cai, D. Liu, J. Yue, M. Ye, Q. Chen and K. Shi, *Intern. Emerg. Med.*, 2021, **16**, 853–862.
20 J. G. Ruiz-Sánchez, I. J. Núñez-Gil, M. Cuesta, M. A. Rubio, C. Maroun-Eid, R. Arroyo-Espliguero, R. Romero, V. M. Becerra-Muñoz, A. Uribarri, G. Feltes, D. Trabattoni, M. Molina, M. García Aguado, M. Pepe, E. Cerrato, E. Alfonso, A. F. Castro Mejía, S. R. Roubin, L. Buzón, E. Bondia, F. Marin, J. López Pais, M. Abumayyaleh, F. D'Ascenzo, E. Rondano, J. Huang, C. Fernandez-Perez, C. Macaya, P. de Miguel Novoa, A. L. Calle-Pascual, V. Estrada Perez and I. Runkle, *Front. Endocrinol.*, 2020, **11**, 1–12.
21 A. A. Tinkov, M. G. Skalnaya, O. P. Ajsuvakova, E. P. Serebryansky, J. C. J. Chao, M. Aschner and A. V. Skalny, *Biol. Trace Elem. Res.*, 2021, **199**, 490–499.
22 N. B. Ivanenko, A. A. Ganeev, N. D. Solovyev and L. N. Moskvin, *J. Anal. Chem.*, 2011, **66**, 784–799.
23 E. V. Skorb, H. Möhwald and D. V. Andreeva, *Adv. Mater. Interfaces*, 2017, **4**, 1600282.
24 N. V. Ryzhkov, A. A. Nikitina, P. Fratzl, C. M. Bidan and E. V. Skorb, *Adv. Mater. Interfaces*, 2021, **8**, 2001807.
25 L. Zhong, J. Ding, J. Qian and M. Hong, *Coord. Chem. Rev.*, 2021, **434**, 213804.
26 L. Liang, L. Liu, F. Jiang, C. Liu, D. Yuan, Q. Chen, D. Wu, H.-L. Jiang and M. Hong, *Inorg. Chem.*, 2018, **57**(9), 4891–4897.
27 L. Liang, Q. Chen, F. Jiang, D. Yuan, J. Qian, G. Lv, H. Xue, L. Liu, H.-L. Jiang and M. Hong, *J. Mater. Chem. A*, 2016, **4**, 15370–15374.
28 J. Ding, L. Zhong, X. Wang, L. Chai, Y. Wang, M. Jiang, T.- Ting Li, Y. Hu, J. Qian and S. Huang, *Sens. Actuators, B*, 2020, **306**, 127551.
29 T. Terse-Thakoor, M. Punjiya, Z. Matharu, B. Lyu, M. Ahmad, G. E. Giles, R. Owyeung, F. Alaimo, M. Shojaei Baghini, T. T. Brunyé and S. Sonkusale, *npj Flexible Electron.*, 2020, **4**, 1–10.
30 A. A. Stekolshchikova, A. V. Radaev, O. Y. Orlova, K. G. Nikolaev and E. V. Skorb, *ACS Omega*, 2019, **4**, 15421–15427.
31 K. G. Nikolaev, E. V. Kalmykov, D. O. Shavronskaya, A. A. Nikitina, A. A. Stekolshchikova, E. A. Kosareva, A. A. Zenkin, I. S. Pantiukhin, O. Y. Orlova, A. V. Skalny and E. V. Skorb, *ACS Omega*, 2020, **5**, 18987–18994.

32 M. P. S. Mousavi, A. Ainla, E. K. W. Tan, M. Abd El-Rahman, Y. Yoshida, L. Yuan, H. H. Sigurslid, N. Arkan, M. C. Yip, C. K. Abrahamsson, S. Homer-Vanniasinkam and G. M. Whitesides, *Lab Chip*, 2018, **18**, 2279–2290.

33 C. Ocaña, M. Muñoz-Correas, N. Abramova and A. Bratov, *Sensors*, 2020, **20**, 1348.

34 N. M. Ivanova, M. B. Levin and K. N. Mikhelson, *Russ. Chem. Bull.*, 2012, **61**, 926–936.

35 I. Š. Ronč̆ević, D. Krivić, M. Buljac, N. Vladislavić and M. Buzuk, *Sensors*, 2020, **20**, 3211.

36 S. Lee, B. Ozlu, T. Eom, D. C. Martin and B. S. Shim, *Biosens. Bioelectron.*, 2020, **170**, 112620.

37 E. V. Skorb, A. V. Volkova and D. V. Andreeva, *Curr. Org. Chem.*, 2015, **19**, 1097–1116.

38 H. Deng, Z. Wang, W. Zhang, B. Hu and S. Zhang, *J. Appl. Polym. Sci.*, 2015, **132**, 1–7.

39 M. Vomero, C. Gueli, E. Zucchini, L. Fadiga, J. B. Erhardt, S. Sharma and T. Stieglitz, *Adv. Mater. Technol.*, 2020, **5**, 1900713.

40 S. Abdu, M. C. Martí-Calatayud, J. E. Wong, M. García-Gabaldón and M. Wessling, *ACS Appl. Mater. Interfaces*, 2014, **6**, 1843–1854.

41 T. Lee, S. H. Min, M. Gu, Y. K. Jung, W. Lee, J. U. Lee, D. G. Seong and B. S. Kim, *Chem. Mater.*, 2015, **27**, 3785–3796.

42 D. V. Andreeva, M. Trushin, A. Nikitina, M. C. F. Costa, P. V. Cherepanov, M. Holwill, S. Chen, K. Yang, S. W. Chee, U. Mirsaidov, A. H. Castro Neto and K. S. Novoselov, *Nat. Nanotechnol.*, 2021, **16**, 174–180.

43 K. Lin, B. Jing and Y. Zhu, *Soft Matter*, 2021, **17**, 8937–8949.

44 S. J. Percival, L. J. Small, E. D. Spoerke and S. B. Rempe, *RSC Adv.*, 2018, **8**, 32992–32999.

45 G. Alfano, A. Ferrari, F. Fontana, R. Perrone, G. Mori, E. Ascione, R. Magistroni, G. Venturi, S. Pederzoli, G. Margiotta, M. Romeo, F. Piccinini, G. Franceschi, S. Volpi, M. Faltoni, G. Ciusa, E. Bacca, M. Tutone, A. Raimondi, M. Menozzi, E. Franceschini, G. Cuomo, G. Orlando, A. Santoro, M. Di Gaetano, C. Puzzolante, F. Carli, A. Bedini, J. Milic, M. Meschiari, C. Mussini, G. Cappelli, G. Guaraldi, C. Mussini, G. Guaraldi, E. Bacca, A. Bedini, V. Borghi, G. Burastero, F. Carli, G. Ciusa, L. Corradi, G. Cuomo, M. Di Gaetano, G. Dolci, M. Faltoni, R. Fantini, G. Franceschi, E. Franceschini, V. Iadisernia, D. Larné, M. Menozzi, M. Meschiari, J. Milic, G. Orlando, F. Pellegrino, A. Raimondi, C. Rogati, A. Santoro, R. Tonelli, M. Tutone, S. Volpi, D. Yaacoub, G. Cappelli, R. Magistroni, G. Alfano, F. Fontana, B. Marco, G. Mori, R. Pulizzi, E. Ascione, M. Leonelli, F. Facchini, F. Damiano, M. Girardis, A. Andreotti, E. Biagioni, F. Bondi, S. Busani, G. Chierego, M. Scotti, L. S. A. Cossarizza, C. Bellinazzi, R. Borella, S. De Biasi, A. De Gaetano, L. Fidanza, L. Gibellini, A. Iannone, D. Lo Tartaro, M. Mattioli, M. Nasi, A. Paolini and M. Pinti, *Clin. Exp. Nephrol.*, 2021, **25**, 401–409.

46 M. A. Zimmer, A. K. Zink, C. W. Weißer, U. Vogt, A. Michelsen, H. J. Priebe and G. Mols, *A&A practice*, 2020, **14**, e01295.

47 Y. Yasui, H. Yasui, K. Suzuki, T. Saitou, Y. Yamamoto, T. Ishizaka, K. Nishida, S. Yoshihara, I. Gohma and Y. Ogawa, *Int. J. Infect. Dis.*, 2020, **100**, 230–236.

48 O. Moreno-Pérez, J.-M. Leon-Ramirez, L. Fuertes-Kenneally, M. Perdiguero, M. Andres, M. Garcia-Navarro, P. Ruiz-Torregrosa, V. Boix, J. Gil, E. Merino, S. Asensio, C. Fernandez, A. Candela, M. Del Mar García, R. Sánchez, S. Reus, P. Ruiz, R. García-Sevila, M.-Á. Martínez, M.-M. García-Mullor, M. Blanes, J. Guijarro, J. C. Pascual, I. Gonzalez, P. Sanso, J. M. Ramos, J. Javaloy, C. Llopis, O. Coronado, E. García, G. Rodríguez, P. Melgar, M. Franco, F. Lluís, C. Zaragoza, C. Alcaraz, A. Carrión, C. Villodre, E. R. De La Cuesta, C. Alenda, F. Peiró, M. Planelles, L. Greco, S. Silvia, A. Francia, I. Verdú, J. Sales, A. Palacios, H. Ballester, A. García-Valentín, M. Márquez, E. Canelo, A. Juan and E. Vives, *Int. J. Infect. Dis.*, 2020, **100**, 449–454.

49 A. Sjöström, S. Rysz, K. Institutet, H. Sjöström and C. Höybye, *Endocr. Connect*, 2021, **10**(7), 805–814.

50 S. Redant, J. Vanderhulst, E. Maillart, R. Attou, A. Gallerani, P. M. Honoré and D. De Bels, *J. Transl. Int. Med.*, 2021, **8**, 255–260.